Heterobimetallic Complexes of Rhenium Containing Bis(dimethylphosphino)methane

Joel T. Mague

Department of Chemistry, Tulane University, New Orleans, Louisiana 70118

Received April 21, 1994[⊗]

The synthesis of the "metalloligand" *fac*-$ReBr(CO)_3(\eta^1$-dmpm$)_2$ (dmpm = bis(dimethylphosphino)methane) (**3**) is reported together with its use for the synthesis of heterobimetallic complexes. With $Cr(CO)_4$(NBD), **3** yields *fac*-$ReBr(CO)_3(\mu$-dmpm$)_2Cr(CO)_4$ (**4**), while with $Mo(CO)_3$(CHT) the product is *fac*-$Re(CO)_3(\mu$-Br$)(\mu$-dmpm$)_2Mo(CO)_3$ (**5**). Reaction of **3** with $Co_2(CO)_8$ forms [*fac*-$Re(CO)_3(\mu$-Br$)(\mu$-dmpm$)_2Co(CO)_2$][$Co(CO)_4$]·MeCN (**6,**) and with [Rh(COD)(acetone)$_x$]OTf a mixture of [*fac*-$Re(CO)_3(\mu$-Br$)(\mu$-dmpm$)_2Rh(CO)$]OTf (**7**) and *fac*-$Re(CO)_3(\mu$-dmpm$)_2Rh(CO)Br_2$ (**8**) results. Complex **3** and $PdCl_2(PhCN)_2$ form *fac*-$Re(CO)_3Br(\mu$-dmpm$)_2PdCl_2$, while with $Pt(C_2H_4)(PPh_3)_2$ the initial product is a mixture of [*fac*-$Re(CO)_3(\mu$-dmpm$)_2Pt(PPh_3)$]Br·H_2O (**12**) and *fac*-$Re(CO)_3(\mu$-dmpm$)_2PtBr$ (**11**). Treatment of this mixture with $NaBPh_4$ converts it all to [*fac*-$Re(CO)_3(\mu$-dmpm$)_2Pt(PPh_3)$]BPh_4 (**10**). The crystal structures of **5**−**8** and **12** have been determined. **5**: Orthorhombic, $P2_12_12_1$; a = 8.5227(8), b = 10.943(1), c = 28.013(2) Å; Z = 4. **6**: Monoclinic, $P2_1/c$; a = 14.006(1), b = 9.1423(9), c = 26.895(2) Å; β = 101.089(5)°; Z = 4. **7**: Triclinic, $P\bar{1}$; a = 11.962(1), b = 13.596(1), c = 9.957(1) Å; α = 99.861(8), β = 103.164(8), γ = 66.216(7)°; Z = 2. **8**: Orthorhombic, $Pca2_1$; a = 12.852(2), b = 13.979(1), c = 14.080(3) Å; Z = 4. **12**: Monoclinic, $P2_1/c$; a = 12.224(2), b = 9.737(1), c = 31.986(5) Å; β = 90.93(1)°; Z = 4.

Introduction

The synthesis and chemistry of heterobimetallic complexes have attracted considerable interest in recent years[1−3] in part by their potential as models for bifunctional catalysts. Among the desirable features of such species are bridging ligands which provide the dimetal core with reasonable flexibility and whose bonds to the metals are not readily cleaved in subsequent reactions. One increasingly successful route to the directed synthesis of specific heterobimetallic complexes is the use of "metalloligands".[2−11] In some of our earlier studies of the "metalloligands" $CpMCl(\eta^1$-$MeN(PF_2)_2)_2$ (M = Fe, Ru)[10,11] and *fac*-$ReBr(CO)_3(\eta^1$-$MeN(PF_2)_2)_2$11 we encountered problems of ligand cleavage and particularly halide transfer to the second metal. To eliminate the first and to further explore how to minimize the second we have begun to study "metalloligands" containing bis(dimethylphosphino)methane (dmpm). We report here on initial results in this area.

Experimental Section

Materials and Measurements. All manipulations were carried out under an atmosphere of purified nitrogen using standard Schlenk techniques. Solvents were appropriately dried and distilled under nitrogen prior to use except for the nitromethane used to obtain the crystal sample of **12**. Literature methods were used to synthesize *fac*-$MBr(CO)_3(MeCN)_2$ (M = Mn, Re),[12] $Cr(CO)_4$(NBD) (NBD = bicyclo-[2.2.1]heptadiene),[13a] $Mo(CO)_3$(CHT) (CHT = cycloheptа-1,3,5-triene),[13b] $[RhCl(COD)]_2$ (COD = cycloocta-1,5-diene),[14] $PdCl_2(PhCN)_2$[15], and $Pt(C_2H_4)(PPh_3)_2$.[16] Bis(dimethylphosphino)methane (dmpm) and other organometallic reagents were purchased from Strem Chemicals. Proton and $^{31}P\{^1H\}$ NMR spectra were obtained on an IBM/Bruker AF-200 spectrometer at 200.132 and 81.015 MHz, respectively. Chemical shifts are referenced to external tetramethylsilane (^1H, δ 0.0) or 85% H_3PO_4 (^{31}P, δ 0.0) with positive shifts downfield of the reference. Infrared spectra were obtained on a Mattson-Cygnus 100 Fourier transform spectrometer. Microanalyses were by Galbraith Laboratories, Knoxville, TN.

***fac*-$MnBr(CO)_3((CH_3)_2PCH_2P(CH_3)_2)$ (1).** A solution of $MnBr(CO)_3(MeCN)_2$ (0.3 g, 0.997 mmol) in 30 mL of dichloromethane plus 2 mL of acetonitrile was transferred via cannula into a solution of dmpm (0.339 g, 2.49 mmol) in dichloromethane. The light, gold-colored solution was stirred at room temperature for 0.5 h, and the solvent and excess ligand were removed in vacuo. Slow concentration of a dichloromethane/hexane solution of the resulting solid under reduced pressure gave yellow orange crystals (yield 0.28 g, 79%). The analytical sample was recrystallized by layering a toluene/dichloromethane solution with hexane. Anal. Calcd for $C_8H_{14}P_2O_3BrMn$: C, 27.06; H, 3.98. Found: C, 27.1; H, 4.2. IR (toluene solution): 2023 (vs), 1954 (vs), 1902 (s) cm^{-1} ($\nu_{C\equiv O}$).[17] ^1H NMR ($CDCl_3$): δ 3.70(dt ($|^2J(H_a-H_b)|$ = 14.5, $|^2J(P-H_a)|$ = 11.2 Hz), 1H, CH_aH_b), 3.07 (dt-($|^2J(H_a-H_b)|$ = 14.5, $|^2J(P-H_b)|$ = 11.0 Hz), 1H, CH_aH_b), δ 1.72 (m, 12H, $P-CH_3$). $^{31}P\{^1H\}$ NMR ($CDCl_3$): δ −3.99 (s).[18]

***fac*-$ReBr(CO)_3((CH_3)_2PCH_2P(CH_3)_2)$ (2).** This was prepared in the same manner as **1** from 0.3 g (0.694 mmol) of $ReBr(CO)_3(MeCN)_2$ and 0.283 g (2.08 mmol) of dmpm. After removal of the volatiles in vacuo the residue was dissolved in acetone and the solution was filtered and diluted with hexane to produce white crystals (yield 0.30 g, 90%).

[⊗] Abstract published in *Advance ACS Abstracts,* August 15, 1994.

(1) Stephan, D. W. *Coord. Chem. Revs.* **1989**, *95*, 41.
(2) Bullock, R. M.; Casey, C. P. *Acc. Chem. Res.* **1987**, *20*, 167.
(3) Chaudret, B.; Delavaux, B.; Poilblanc, R. *Coord. Chem. Revs.* **1988**, *86*, 191.
(4) Carr, S. W.; Fontaine, X. L. R.; Shaw, B. L.; Thornton-Pett, M. *J. Chem. Soc., Dalton Trans.* **1988**, 769 and references therein.
(5) Blagg, A.; Pringle, P. G.; Shaw, B. L. *J. Chem. Soc., Dalton Trans.* **1987**, 1495 and references therein.
(6) Ferguson, G. S.; Wolczanski, P. I.; Parkanyi, L.; Zonnevylle, M. C. *Organometallics* **1988**, *7*, 1967.
(7) Fontaine, X. L. R.; Jacobson, G. B.; Shaw, B. L.; Thorton-Pett, M. *J. Chem. Soc., Dalton Trans.* **1988**, 741 and referenes therein.
(8) Mague, J. T.; Johnson, M. P. *Organometallics* **1990**, *9*, 1254.
(9) Mague, J. T. *Organometallics* **1991**, *10*, 513.
(10) Mague, J. T.; Lin, Z. *Organometallics* **1992**, *11*, 4139.
(11) Mague, J. T.; Lin, Z. *Organometallics*, in press.
(12) Farona, M. F.; Kraus, K. F. *Inorg. Chem.* **1970**, *9*, 1700.
(13) (a) King, R. B. *Organometallic Syntheses*; Academic Press: New York, 1965; Vol. 1, p 122. (b) *Ibid.,* p 125.
(14) Mague, J. T.; Lloyd, C. L. *Organometallics* **1988**, *7*, 983.
(15) Doyle, J. R.; Slade, P. E.; Jonassen, H. B. *Inorg. Synth.* **1960**, *6*, 218.
(16) Nagel, U. *Chem. Ber.* **1982**, *115*, 1998.
(17) Key to infrared band intensities: vs, very strong; s, strong; m, medium; sh, shoulder.
(18) Key to NMR peak multiplicities: s, singlet; d, doublet; dt, doublet of triplets; td, triplet of doublets; vir t, "virtual triplet"; m, multiplet; br, broad.

0020-1669/94/1333-4261$04.50/0

The analytical sample was recrystallized in the same manner as for **1**. Anal. Calcd for $C_8H_{14}P_2O_3BrRe$: C, 19.76; H, 2.91. Found: C, 19.9; H, 3.0. IR (CH_2Cl_2 solutionn): 2029 (vs), 1946 (vs), 1898 (s) cm^{-1} ($\nu_{C\equiv O}$). ^1H NMR ($CDCl_3$): δ 3.84 (dt ($|^2J(H_a-H_b)|$ = 14.9, $|^2J(P-H_a)|$ = 9.7 Hz), 1H, CH_aH_b), 3.68 (dt($|^2J(H_a-H_b)|$ = 14.9, $|^2J(P-H_b)|$ = 11.2 Hz), 1H, CH_aH_b), 1.84 (vir t, 6H, P—CH_3), 1.74 (vir t, 6H, P—CH_3). $^{31}P\{^1H\}$ NMR($CDCl_3$): δ −64.0 (s).

***fac*-ReBr(CO)$_3$(η^1-(CH$_3$)$_2$PCH$_2$P(CH$_3$)$_2$)$_2$ (3).** To a suspension of 0.3 g (0.694 mmol) of $ReBr(CO)_3(MeCN)_2$ in 10 mL of toluene was added 0.293 g (2.08 mmol) of dmpm and the solution maintained at gentle reflux overnight. Removal of the volatiles in vacuo yielded a colorless oil which could not be induced to crystallize. Because of its air-sensitivity, satisfactory analyses could not be obtained, but from the NMR spectra of the oil the product was generally 90−95% pure with the remainder being a small amount of **2**. IR (hexane solutionn): 2033 (s), 1956 (m), 1900 (vs) cm^{-1} ($\nu_{C\equiv O}$). ^1H NMR (C_6D_6): δ 1.87 (m, 4H, CH_2), 1.56 (vir t, 3H, P—CH_3), 1.47 (vir t, 3H, P—CH_3), 0.80 (d|^2(J(P−H)| = 6.02 Hz), 3H, P—CH_3), 0.78 (d($|^2J$(P−H)| = 6.12 Hz), 3H, P—CH_3). $^{31}P\{^1H\}$ NMR (C_6D_6): AA′XX′ pattern, $\delta(P_A)$ −37.0, $\delta(P_X)$ −59.7, J(AX) = 43.7, J(AX′) = 1.1, J(AA′) = 30.2, J(XX′) = 0 Hz.

***fac*-Re(CO)$_3$Br(μ-(CH$_3$)$_2$PCH$_2$P(CH$_3$)$_2$)$_2$Cr(CO)$_4$ (4).** To a toluene solution (5 mL) of *ca.* 0.46 mmol of **3**, prepared in situ, was added 0.096 g (0.46 mmol) of solid $Cr(CO)_4(NBD)$, and the mixture was stirred overnight at room temperature resulting in the formation of a yellow solid. As the ^{31}P NMR spectrum of the supernatant showed a significant amount of unreacted **3**, the reaction mixture was heated at 90 °C for 0.5 h. After cooling, the solution was diluted with diethyl ether and the yellow solid filtered off and extracted with acetone. Dilution of the acetone extract with diethyl ether and cooling at −10 °C gave the product as yellow crystals (yield 0.14 g, 40%). Anal. Calcd for $C_{17}H_{28}P_4O_7BrCrRe$: C, 25.96; H, 3.60. Found: C, 26.0; H, 3.7. IR (CH_2Cl_2 solution): 2035 (m), 2010 (m), 1954 (m), 1914 (sh), 1902 (vs), 1881 (sh) cm^{-1} ($\nu_{C\equiv O}$). ^1H NMR (d_6-acetone): δ 2.84 (m, 4H, CH_2), 2.07 (vir t, 6H, P—CH_3), 2.00 (vir t, 6H, P—CH_3), 1.82 (vir t, 6H, P—CH_3), 1.73 (vir t, 6H, P—CH_3). $^{31}P\{^1H\}$ NMR (d_6-acetone): AA′XX′ pattern, $\delta(P_A)$ 15.7, $\delta(P_X)$, −35.8; J(AA′) = 28.4, J(AX) = 14.5, J(AX′) = 0.2, J(XX′) = 22.0 Hz.

***fac*-Re(CO)$_3$(μ-Br)(μ-(CH$_3$)$_2$PCH$_2$P(CH$_3$)$_2$)$_2$Mo(CO)$_3$ (5).** To a solution of *ca.* 0.46 mmol of **3**, prepared in situ, in 5 mL of tetrahydrofuran was added 0.125 g (0.46 mmol) of solid $Mo(CO)_3$-(CHT). After being stirred for several minutes at room temperature, the initial dark red solution had lightened and a yellow solid formed. The reaction mixture was diluted with 2 mL of diethyl ether and cooled at −10 °C. Filtration of the solid followed by washing with acetone/diethyl ether and drying in vacuo afforded the product as yellow crystals (yield 0.31 g, 85%). Anal. Calcd for $C_{16}H_{28}P_4O_6BrMoRe$: C, 23.95; H, 3.52. Found: C, 24.2; H, 3.6. IR (acetone solution): 2035 (s), 1952 (m), 1931 (vs), 1911 (m), 1838 (m), 1798 (m) cm^{-1} ($\nu_{C\equiv O}$). ^1H NMR (d_6-acetone): δ 2.43 (m, 2H, CH_2), 2.15 (m, 2H, CH_2), 1.89 (vir t, 6H, P—CH_3), 1.71 (vir t, 6H, P—CH_3), 1.56 (vir t, 6H, P—CH_3). $^{31}P\{^1H\}$ NMR (d_6-acetone): AA′XX′ pattern $\delta(P_A)$ − 6.02, $\delta(P_X)$ −35.3.

[*fac*-Re(CO)$_3$(μ-Br)(μ-(CH$_3$)$_2$PCH$_2$P(CH$_3$)$_2$)$_2$Co(CO)$_2$][Co-(CO)$_4$]·CH$_3$CN (6). To a solution of *ca.* 0.68 mmol of **3**, prepared in situ, in 5 mL of toluene was added 0.23 g (0.68 mmol) of $Co_2(CO)_8$ dissolved in 5 mL of toluene. Gas evolution was immediate, and an oily brown solid formed. At the end of the addition of the $Co_2(CO)_8$ solution some lighter colored solid also appeared to be present. After being stirred for 3 h at room temperature, the solution had darkened somewhat and much solid was present. The solid was filtered out and washed with toluene. The residual solid was extracted with acetone and the extract diluted with diethyl ether. On cooling at −10 °C orange crystals formed. The supernatant was syringed off, and the crystals were washed with diethyl ether containing a small amount of acetone. Recrystallization from acetonitrile/diethyl ether afforded the product as orange needles (yield 0.34 g, 53%). Anal. Calcd for $C_{21}H_{31}O_9P_4NBrCo_2Re$: C, 26.57; H, 3.30. Found: C, 25.7; H, 3.0. IR (acetone solution): 2041 (m), 2029 (sh), 2006 (m), 1958 (m), 1929 (s), 1892 (vs) cm^{-1} ($\nu_{C\equiv O}$). ^1H NMR (d_6-acetone): 3.35 (m, 2H, CH_2), 2.87 (m, 2H, CH_2), 2.11 (vir t, 6H, P—CH_3), 2.03 (m, 12H, P—CH_3), 1.89 (vir t, 6H, P—CH_3). $^{31}P\{^1H\}$ NMR (d_6-acetone): $\delta(P_{Co})$ 27.1(s), $\delta(P_{Re})$ −21.0(s).

[*fac*-Re(CO)$_3$(μ-Br)(μ-(CH$_3$)$_2$PCH$_2$P(CH$_3$)$_2$)$_2$Rh(CO)][CF$_3$SO$_3$] (7). An acetone solution of $[RhCl(COD)]_2$ (0.113 g, 0.23 mmol) was treated with 0.118 g (0.46 mmol) of solid silver trifluoromethanesulfonate, and the mixture was stirred for 0.5 h. Following filtration through a pad of diatomaceous earth to remove the precipitated AgCl, a solution of **3**, prepared in situ, in 2.5 mL of toluene (*ca.* 0.46 mmol) was added to the filtrate and the mixture was stirred at room temperature overnight. Bubbling CO through the resulting orange solution caused an initial color change to dark red followed by a reversion to bright orange. Dilution with diethyl ether and cooling resulted in the formation of a mixture of yellow and red orange crystals. These were filtered off, washed with diethyl ether containing a small amount of acetone, and dried in vacuo. Extraction of the solid with acetone followed by slow crystallization by vapor diffusion of diethyl ether into the acetone solution afforded the product as large yellow crystals which were hand-separated from a small quantity of the red orange crystals (yield 0.3 g, 70%) Anal. Calcd for $C_{16}H_{28}O_8P_4F_3SBrRhRe$: C, 20.65; H, 3.04; Br, 8.59. Found: C, 20.2; H, 3.1; Br, 8.5. IR (acetone solution): 2041 (vs), 1992 (s), 1960 (s), 1927 (vs) cm^{-1} ($\nu_{C\equiv O}$). ^1H NMR (d_6-acetone): δ 3.58 (m, 2H, CH_2), 2.99 (m, 2H, CH_2), 2.35 (vir t, 6H, P—CH_3), 2.01 (vir t, 6H, P—CH_3), 1.83 (m, 12H, P—CH_3). $^{31}P\{^1H\}$ NMR (d_6-acetone): $\delta(P_{Rh})$ −4.34 (dt(^1J(Rh−P) = 107.8, J(P−P′) = 10.7 Hz), $\delta(P'_{Re})$ −31.0 (td(J(P−P′) = 10.7, J(P′−Rh) = 3.5 Hz).

***fac*-ReBr(CO)$_3$(μ-(CH$_3$)$_2$PCH$_2$P(CH$_3$)$_2$)$_2$PdCl$_2$ (9).** To a solution of 0.176 g (0.46 mmol) of $PdCl_2(NCPh)_2$ in 10 mL of toluene was added a toluene solution of *ca.* 0.46 mmol of **3** which had been prepared in situ. The color of the solution immediately lightened, and an off-white precipitate formed. After the mixture was stirred for 2 h, the solid was filtered off, washed with diethyl ether, and dried in vacuo. The yield was essentially quantitative, and the product was too insoluble to be recrystallized or to obtain an NMR spectrum. Anal. Calcd for $C_{13}H_{28}O_3P_4Cl_2BrPdRe$: C, 19.52; H, 3.54. Found: C, 20.1; H, 3.8. IR (Nujol mull): 2031 (vs), 1946 (s), 1894 (s) cm^{-1} ($\nu_{C\equiv O}$).

[*fac*-Re(CO)$_3$(μ-(CH$_3$)$_2$PCH$_2$P(CH$_3$)$_2$)$_2$Pt(P(C$_6$H$_5$)$_3$)]B-(C$_6$H$_5$)$_4$·0.5CH$_2$Cl$_2$ (10). To a solution of 0.311 g (0.46 mmol) of Pt-$(C_2H_4)(PPh_3)_2$ in 5 mL of ethylene-saturated dichloromethane was added *ca.* 0.46 mmol of **3**, prepared in situ, in 5 mL of toluene. The solution immediately became a cloudy orange color, and after being stirred for 10 min at room temperature, it was filtered through a pad of diatomaceous earth. Concentration of the filtrate in vacuo followed by dilution with diethyl ether and cooling afforded an orange-yellow, microcrystalline solid. This was filtered off and dissolved in 5 mL of methanol. Addition of slightly more than 1 equiv of sodium tetraphenylborate in 2 mL of methanol resulted in the immediate precipitation of an orange solid. This was filtered off, washed with methanol, and recrystallized from dichloromethane/methanol as dull orange crystals (yield 0.52 g, 85%). Anal. Calcd for $C_{55.5}H_{64}P_5O_3BClRePt$: C, 48.95; H, 4.75. Found: C, 48.9; H, 4.7$_5$. IR (Nujol mull): 1985 (vs), 1894 (vs) cm^{-1} ($\nu_{C\equiv O}$). ^1H NMR ($CDCl_3$): δ 6.82−7.59 (m, 35H, C_6H_5), 3.06 (br, 2H, CH_2), 2.90 (br, 2H, CH_2), 1.66 (vir t, 6H, P—CH_3), 1.37 (vir t, 6H, P—CH_3), 0.86 (M, 12H, P—CH_3). $^{31}P\{^1H\}$ NMR ($CDCl_3$): $\delta(PPh_3)$ 18.8 (m(^1J(Pt−P) = 1714.6, ^2J(P−P′) = 22.0, J(P−P″) = 22.2 Hz)), $\delta(P'_{Pt})$ −15.3 (m(^1J(Pt−P′) = 3030.3, ^2J(P′−P) = 22.0, J(P′−P″) = 39.3 Hz)), $\delta(P''_{Re})$ −39.8 (m(J(P″−P) = 22.2, J(P″−P′) = 39.3 Hz)).

X-ray Crystallography. General procedures for crystal orientation, unit cell determination, refinement, and data collection on the Enraf-Nonius CAD-4 diffractometer have been published.[14] Details specific to the present study are given in Table 1. All crystals were mounted on thin glass fibers and coated with epoxy cement. Crystal systems and unit cells obtained by the CAD-4 software were confirmed by observation of the appropriate diffraction symmetry. The space groups for **5**, **6**, **8**, and **12** were uniquely determined by the systematic absences in the final data sets. All data sets were corrected for Lorentz and polarization effects and for absorption by employing ψ scans on several reflections with χ near 90° except for **5** in which an empirical correction (DIFABS[19]) was used. Metal atom positions were obtained from origin-removed Patterson functions and the structures developed by

(19) Walker, N.; Stuart, D. *Acta Crystallogr.* **1983**, *A39*, 158.

Table 1. Summary of Crystallographic Data

	5	6	7	8	12
formula	$C_{16}H_{28}P_4O_6BrMoRe$	$C_{21}H_{31}O_9P_4NBrCo_2Re$	$C_{16}H_{28}O_8P_4F_3SBrRhRe$	$C_{14}H_{28}P_4O_4Br_2RhRe$	$C_{31}H_{45}P_5O_4BrRePt$
fw	802.34	949.35	930.37	833.20	1097.77
space group	$P2_12_12_1$ (No. 19)	$P2_1/c$ (No. 14)	$P\bar{1}$ (No. 2)	$Pca2_1$ (No. 29)	$P2_1/c$ (No. 14)
a, Å	8.5227(8)	14.006(1)	11.692(1)	12.852(2)	12.224(2)
b, Å	10.943(1)	9.1423(9)	13.596(1)	13.979(1)	9.737(1)
c, Å	28.013(2)	26.895(2)	9.957(1)	14.080(3)	31.986(5)
α, deg			99.861(8)		
β, deg		101.089(5)	103.164(8)		90.93(1)
γ, deg			66.216(7)		
V, Å^3	2612.7(7)	3379.7(8)	1437.2(4)	2530(1)	3807(2)
Z	4	4	2	4	4
ϱ_{calc}, g cm^{-3}	2.04	1.87	2.15	2.19	1.92
μ, cm^{-1}	69.4	59.5	65.5	88.9	82.1
range trans factors	0.8878–1.4293	0.5347–0.9965	0.4551–0.9977	0.6627–0.9995	0.3590–0.9983
temp, K	293	293	293	293	293
radtn	Mo Kα (graphite monochromated, λ = 0.710 73 Å)				
R^a	0.027	0.027	0.028	0.033	0.029
$R_w{}^b$	0.036	0.037	0.039	0.043	0.039

$^a R = \Sigma||F_o| - |F_c||/\Sigma|F_o|$. $^b R_w = [\Sigma w(|F_o| - |F_c|)^2/\Sigma w(|F_o|)^2]^{1/2}$ with $w = 1/(\sigma_F)^2$; $\sigma_F = \sigma(F^2)/2F$; $\sigma(F^2) = [(\sigma_I)^2 + (0.04F^2)^2]^{1/2}$.

successive cycles of full-matrix, least-squares refinement followed by calculation of a $\Delta\varrho$ map. The neutral atom scattering factors used include correction for the real and imaginary components of the effect of anomalous dispersion.[20] In the final cycles, many hydrogen atoms were visible in $\Delta\varrho$ maps. These were included as fixed contributions in idealized positions (C–H = 0.95 Å) with isotropic thermal displacement parameters 20% larger than those of the attached carbon atoms and updated periodically. All calculations were performed on a VAXstation 3100 with the MolEN suite of programs.[21]

(a) *fac*-Re(CO)$_3$(μ-Br)(μ-dmpm)$_2$Mo(CO)$_3$ (5). The crystal used was a bright yellow, octahedral wedge obtained by layering an acetone solution of the complex with hexane. Only statistical fluctuations were seen in the intensities of three monitor reflections. Following solution and refinement of the initial model, the opposite enantiomorph was refined to convergence. This resulted in a significant (>98% confidence level) improvement in R and R_w and so was taken to be the correct model.

(b) [*fac*-Re(CO)$_3$(μ-Br)(μ-dmpm)$_2$Co(CO)$_2$][Co(CO)$_4$]·MeCN (6). An orange needle, obtained by slow vapor diffusion of diethyl ether into an acetonitrile solution of the complex, was cut to give a suitably sized fragment. The data were additionally corrected for an 8.6% anisotropic decay in the intensities of the monitor reflections. In the late stages of the refinement, a linear region of electron density appeared in the $\Delta\varrho$ map which was taken to be a molecule of solvent acetonitrile. The geometry obtained following initial refinement suggested an end-to-end disorder, but it proved impossible to determine occupancies for the two orientations so a single orientation was assumed with the thermal parameters of the terminal atoms allowed to refine without constraints to accommodate the disorder.

(c) [*fac*-Re(CO)$_3$(μ-Br)(μ-dmpm)$_2$Rh(CO)]OTf (7). A yellow block, obtained from vapor diffusion of diethyl ether into a solution of the crude complex in dichloromethane/acetone, was used. Only statistical fluctuations were observed in the intensities of the monitor reflections. As a reasonable density suggested $Z = 2$, $P\bar{1}$ was chosen initially, and although a reasonable fragment consisting of the metal atoms and the bromine could be deduced from the Patterson map, further development of the structure could not be accomplished in $P1$. Therefore a fragment consisting of these atoms plus two phosphorus atoms on rhenium was used to calculate structure factors in $P1$ from which portions of a second molecule could be obtained. Further development and refinement in this space group enabled most non-hydrogen atoms to be located, and it soon became clear that the two molecules were related by a center of symmetry. Returning one of these to $P\bar{1}$ allowed completion and refinement of the model to proceed without further difficulty indicating the choice of the centrosymmetric space group to be correct.

(d) *fac*-Re(CO)$_3$(μ-dmpm)$_2$Rh(CO)Br$_2$ (8). A dark orange crystal, obtained as an impurity in the sample of crystals from which **7** was the major component, was used. Only statistical fluctuations were noted in the intensities of the monitor reflections. Following refinement of the initial model, the opposite enantiomorph was refined to convergence which resulted in a significant (>98% confidence level) improvement in R and R_w so the latter was taken to be the correct model.

(e) [*fac*-Re(CO)$_3$(μ-dmpm)$_2$Pt(PPh$_3$)]Br·H$_2$O (12). A yellow orange plate, obtained by the slow diffusion of diethyl ether into a nitromethane solution of the crude material obtained from the reaction of **3** with Pt(C$_2$H$_4$)(PPh$_3$)$_2$, was cut to size. The data were additionally corrected for a linear 3.6% decrease in the intensities of the monitor reflections. In the late stages of the refinement a single peak in the $\Delta\varrho$ map having a peak height comparable to that seen previously for the carbonyl oxygen atoms was found. This was taken to be the oxygen atom of a water molecule, presumably derived from moisture in the nitromethane which had not been dried, and although attached hydrogen atoms could not be definitively located, its reasonable refinement supports the choice.

Final refined atomic coordinates are given in Tables 2–6, and additional crystallographic data are supplied as supplementary material.

Results and Discussion

Preparation of Complexes. Reaction of a 3-fold excess of dmpm with *fac*-MBr(CO)$_3$(MeCN)$_2$ (M = Mn, Re) at room temperature afforded yellow orange and white crystals, respectively, which analyze as MnBr(CO)$_3$(dmpm) (**1**) and ReBr(CO)$_3$-

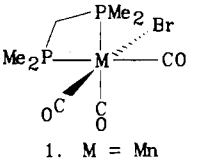

1. M = Mn
2. M = Re

(dmpm) (**2**). The observation of "virtual triplet" resonances for the phosphine methyl groups in **2**, generally considered to be the result of strong P–P coupling, initially suggested a dinuclear species with *trans*-disposed phosphorus atoms. However, crystal structure determinations[22] showed both **1** and **2** to be monomeric with a chelating dmpm ligand. Evidently the combined effects of ^2J(P–Re–P) and ^2J(P–C–P) are large

(20) (a) Cromer, D. T.; Waber, J. T. *International Tables for X-ray Crystallography*; The Kynoch Press, Birmingham, England, 1974; Vol. IV, Table 2.2.B. (b) Cromer, D. T. *Ibid.*, Table 3.2.1.

(21) Fair, C. K. MolEN, *An Interactive Intelligent System for Crystal Structure Analysis*; Enraf-Nonius: Delft, The Netherlands, 1990.

(22) Mague, J. T. *Acta Crystallogr.* **1994**, *C50*, in press.

Table 2. Positional and Thermal Parameters (Esd's in Parentheses) for $Re(CO)_3(\mu\text{-}Br)(\mu\text{-}dmpm)_2Mo(CO)_3$ (**5**)

atom	*x*	*y*	*z*	B_{eq}[a] Å^2
Re	0.74174(5)	−0.09847(3)	0.93052(1)	1.982(6)
Mo	0.6568(1)	0.24808(8)	0.83983(3)	1.91(1)
Br	0.5699(1)	0.0989(1)	0.91401(4)	2.54(2)
P(1)	1.0032(3)	−0.0008(3)	0.9215(1)	2.93(6)
P(2)	0.9129(3)	0.2680(3)	0.8844(1)	2.44(5)
P(3)	0.7140(3)	−0.1503(2)	0.84562(9)	2.05(5)
P(4)	0.7609(3)	0.0879(2)	0.78363(8)	1.96(4)
O(1)	0.737(1)	−0.0202(9)	1.0362(3)	5.1(2)
O(2)	0.443(1)	−0.2516(8)	0.9460(3)	4.5(2)
O(3)	0.913(1)	−0.3362(8)	0.9498(3)	5.3(2)
O(4)	0.765(1)	0.4264(7)	0.7613(3)	3.9(2)
O(5)	0.3267(9)	0.2279(9)	0.7917(3)	4.6(2)
O(6)	0.525(1)	0.4772(8)	0.8941(4)	5.8(2)
C(1)	0.739(1)	−0.049(1)	0.9975(4)	3.0(2)
C(2)	0.548(1)	−0.190(1)	0.9407(4)	3.0(2)
C(3)	0.852(1)	−0.243(1)	0.9428(4)	3.3(2)
C(4)	0.719(1)	0.3598(9)	0.7900(4)	2.4(2)
C(5)	0.449(1)	0.233(1)	0.8105(4)	3.0(2)
C(6)	0.576(1)	0.390(1)	0.8756(4)	3.1(2)
C(7)	1.149(1)	−0.106(1)	0.8963(6)	5.3(3)
C(8)	1.095(2)	0.031(1)	0.9789(5)	5.1(3)
C(9)	1.051(1)	0.138(1)	0.8864(4)	2.5(2)
C(10)	0.900(2)	0.315(1)	0.9460(4)	4.5(3)
C(11)	1.046(2)	0.383(1)	0.8607(5)	4.6(3)
C(12)	0.513(1)	−0.141(1)	0.8243(4)	3.1(2)
C(13)	0.766(2)	−0.3087(9)	0.8340(4)	3.8(2)
C(14)	0.826(1)	−0.0690(8)	0.7986(4)	2.3(2)
C(15)	0.633(2)	0.057(1)	0.7331(4)	3.6(3)
C(16)	0.936(2)	0.138(1)	0.7518(4)	3.4(2)

[a] *B* values for anisotropically refined atoms are given in the form of the isotropic equivalent displacement parameter defined as $B_{eq} = (8\pi^2/3)\sum_i\sum_j U_{ij}a^*_i a^*_j \mathbf{a}_i\cdot\mathbf{a}_j$.

enough to cause this effect, and we note that the same phenomenon occurs for the methyl groups attached to the coordinated phosphorus atoms in **3** (vide infra) and in *cis*-$Cr(CO)_4$(dmpm).[23] The remaining spectroscopic data for **1** and **2** are in accord with the structures established by X-ray crystallography.

If *fac*-$ReBr(CO)_3(MeCN)_2$ is heated with a 3-fold excess of dmpm in toluene overnight, substantially complete conversion to *fac*-$ReBr(CO)_3(\eta^1\text{-dmpm})_2$ (**3**) occurs. Complex **3** is obtained

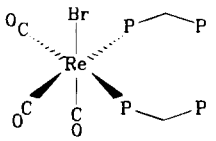

3

as a colorless, air-sensitive oil on removal of the volatiles in vacuo. Because of its air-sensitivity, satisfactory elemental analysis could not be obtained for **3**, but its composition and structure are well-established by the spectroscopic data and by its subsequent chemistry. Thus the infrared spectrum consists of three absorptions in the carbonyl stretching region which are at similar energies as those for **2** indicating the presence of the *fac*-{$Re(CO)_3$} unit. The $^{31}P\{^1H\}$ NMR spectrum consists of two resonances of equal intensity which can be satisfactorily analyzed as an AA′XX′ spin system. The higher field resonance occurs close to the chemical shift of free dmpm (δ −56.5) and is thus assigned to the uncoordinated phosphorus atoms. The proton NMR spectrum shows the methyl groups on each coordinated phosphorus atom to be nonequivalent, consistent with the proposed structure, and to also exhibit the effects of "virtual" coupling.

(23) King, R. B.; Raghuveer, K. S. *Inorg. Chem.* **1984**, *23*, 2482.

Table 3. Positional and Thermal Parameters (Esd's in Parentheses) for $[Re(CO)_3(\mu\text{-}Br)(\mu\text{-}dmpm)_2Co(CO)_2][Co(CO)_4]\cdot MeCN$ (**6**)

atom	*x*	*y*	*z*	B_{eq},[a] Å^2
Re	0.01290(2)	0.09529(2)	0.36622(1)	2.845(4)
Br	0.16900(4)	0.12374(6)	0.32625(2)	3.11(1)
Co(1)	0.19297(5)	0.38842(8)	0.31436(3)	2.83(1)
P(1)	0.0837(1)	0.2763(2)	0.43053(5)	2.98(3)
P(2)	0.2729(1)	0.3940(2)	0.39383(5)	3.07(3)
P(3)	−0.0750(1)	0.2557(2)	0.29898(6)	3.62(3)
P(4)	0.0887(1)	0.3713(2)	0.24121(6)	3.43(3)
O(1)	0.1172(4)	−0.1417(5)	0.4387(2)	6.3(1)
O(2)	−0.0660(4)	−0.1597(5)	0.2943(2)	6.3(1)
O(3)	−0.1654(4)	0.0747(6)	0.4156(2)	7.2(1)
O(4)	0.1171(4)	0.6719(5)	0.3307(2)	5.2(1)
O(5)	0.3702(3)	0.3938(6)	0.2722(2)	6.3(1)
C(1)	0.0804(4)	−0.0507(7)	0.4125(2)	3.7(1)
C(2)	−0.0348(4)	−0.0635(7)	0.3200(2)	3.9(1)
C(3)	−0.0976(4)	0.0830(7)	0.3963(2)	4.1(1)
C(4)	0.1420(4)	0.5536(7)	0.3255(2)	3.8(1)
C(5)	0.2999(4)	0.3844(6)	0.2876(2)	3.7(1)
C(6)	0.2156(4)	0.2943(6)	0.4392(2)	3.0(1)
C(7)	0.0716(5)	0.2164(8)	0.4935(2)	4.7(1)
C(8)	0.0387(4)	0.4628(7)	0.4300(2)	3.9(1)
C(9)	0.3931(4)	0.3109(9)	0.4030(2)	4.9(2)
C(10)	0.2962(5)	0.5732(7)	0.4231(2)	4.3(1)
C(11)	−0.0199(4)	0.2616(7)	0.2425(2)	4.0(1)
C(12)	−0.1075(5)	0.4441(8)	0.3097(3)	4.9(2)
C(13)	−0.1937(5)	0.179(1)	0.2728(3)	6.1(2)
C(14)	0.1363(5)	0.2839(8)	0.1903(2)	5.1(2)
C(15)	0.0413(6)	0.5402(8)	0.2119(3)	6.0(2)
Co(2)	0.82278(7)	0.0534(1)	0.09813(3)	5.08(2)
O(16)	0.9086(5)	−0.1442(9)	0.1786(2)	11.3(2)
O(17)	0.7352(6)	0.2945(8)	0.1417(3)	15.0(2)
O(18)	0.9617(5)	0.166(1)	0.0405(2)	10.8(2)
O(19)	0.6823(4)	−0.1250(7)	0.0316(2)	7.9(2)
C(16)	0.8770(6)	−0.064(1)	0.1469(3)	6.7(2)
C(17)	0.7690(7)	0.200(1)	0.1244(3)	8.7(3)
C(18)	0.9080(6)	0.120(1)	0.0646(3)	6.8(2)
C(19)	0.7369(5)	−0.0519(9)	0.0573(3)	5.3(2)
C(1s)	0.6220(9)	0.090(2)	0.4562(5)	14.5(5)
C(2s)	0.6305(8)	0.064(1)	0.5062(7)	14.2(5)
N	0.6330(8)	0.047(1)	0.5525(5)	14.5(4)

[a] *B* values for anisotropically refined atoms are given in the form of the isotropic equivalent displacement parameter defined as $B_{eq} = (8\pi^2/3)\sum_i\sum_j U_{ij}a^*_i a^*_j \mathbf{a}_i\cdot\mathbf{a}_j$.

Attempts to prepare the manganese analog of **3** failed to give any characterizable product.

Reaction of **3** with $Cr(CO)_4$(NBD) occurs slowly at room temperature and more rapidly on heating to give yellow, sparingly soluble crystals (**4**). The analytical data are consistent

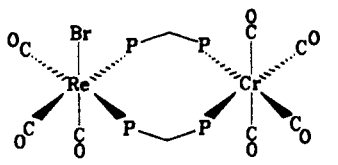

4

with formulation of **4** as either $ReBrCr(CO)_7(dmpm)_2$ or $ReBrCr(CO)_6(dmpm)_2$ with the latter expected to have a structure like **5** (vide infra). The infrared spectrum supports

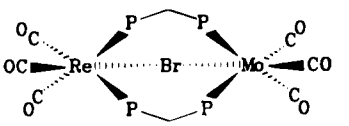

5

the formulation $ReBrCr(CO)_7(dmpm)_2$, which is proposed to contain *fac*-{$Re(CO)_3$} and *cis*-{$Cr(CO)_4$} units. In particular,

Table 4. Positional and Thermal Parameters (Esd's in Parentheses) for $[Re(CO)_3(\mu\text{-}Br)(\mu\text{-}dmpm)_2Rh(CO)]OTf$ (**7**)

atom	*x*	*y*	*z*	B_{eq}[a] Å^2
Re	0.00191(1)	0.24040(1)	0.05613(2)	2.043(4)
Rh	−0.10383(3)	0.22501(3)	0.38462(4)	2.338(8)
Br	−0.04818(4)	0.10240(4)	0.17018(5)	2.78(1)
P(1)	−0.1983(1)	0.3872(1)	0.0932(1)	2.48(3)
P(2)	−0.3074(1)	0.2941(1)	0.2720(1)	2.78(3)
P(3)	0.1431(1)	0.2674(1)	0.2700(1)	2.57(3)
P(4)	0.1023(1)	0.1521(1)	0.4870(1)	2.68(3)
O(1)	0.0572(4)	0.3960(3)	−0.0812(4)	5.1(1)
O(2)	−0.1383(4)	0.1778(4)	−0.2246(5)	5.2(1)
O(3)	0.2376(4)	0.0589(4)	−0.0303(5)	5.2(1)
O(4)	−0.1677(5)	0.3759(4)	0.6299(5)	5.9(1)
C(1)	0.0351(4)	0.3360(4)	−0.0272(5)	2.7(1)
C(2)	−0.0915(5)	0.2024(4)	−0.1184(6)	3.1(1)
C(3)	0.1500(5)	0.1251(4)	0.0062(5)	3.0(1)
C(4)	−0.1428(5)	0.3161(5)	0.5364(6)	3.5(1)
C(5)	0.2848(5)	0.2662(5)	0.2303(7)	4.5(1)
C(6)	0.1004(5)	0.3891(4)	0.3869(6)	3.7(1)
C(7)	0.2069(4)	0.1578(4)	0.3820(5)	2.9(1)
C(8)	0.1613(6)	0.0115(5)	0.5171(8)	5.0(2)
C(9)	0.1501(6)	0.2131(6)	0.6555(6)	4.9(2)
C(10)	−0.2718(5)	0.4642(5)	−0.0580(6)	4.0(1)
C(11)	−0.2055(5)	0.4938(5)	0.2306(6)	3.8(1)
C(12)	−0.3204(4)	0.3422(5)	0.1060(6)	3.5(1)
C(13)	−0.3827(5)	0.1981(5)	0.2227(7)	4.4(1)
C(14)	−0.4164(5)	0.4067(6)	0.3612(7)	4.9(2)
S	0.4944(2)	0.7388(2)	0.3403(2)	4.64(4)
O(5)	0.4711(6)	0.6618(5)	0.2358(8)	9.0(2)
O(6)	0.6200(4)	0.7095(5)	0.4049(6)	6.5(2)
O(7)	0.4086(6)	0.7866(8)	0.4317(7)	12.1(3)
C(15)	0.4651(7)	0.8492(7)	0.2448(9)	6.6(2)
F(1)	0.5389(5)	0.8192(6)	0.1527(7)	12.1(2)
F(2)	0.4907(7)	0.9277(5)	0.322(1)	13.7(3)
F(3)	0.3507(5)	0.8886(4)	0.1800(6)	9.9(2)

[a] *B* values for anisotropically refined atoms are given in the form of the isotropic equivalent displacement parameter defined as $B_{eq} = (8\pi^2/3)\sum_i\sum_j U_{ij}a^*_i a^*_j \mathbf{a}_i\cdot\mathbf{a}_j$.

Table 5. Positional and Thermal Parameters (Esd's in Parentheses) for $Re(CO)_3(\mu\text{-}dmpm)_2Rh(CO)Br_2$ (**8**)

atom	*x*	*y*	*z*	B_{eq},[a] Å^2
Re	0.06664(4)	0.17243(4)	0.400	2.448(8)
Rh	−0.09090(*)	0.29969(7)	0.32540(9)	2.08(2)
Br(1)	−0.2313(1)	0.3860(1)	0.2086(1)	3.61(3)
Br(2)	−0.1096(2)	0.4162(2)	0.4597(2)	5.31(5)
P(1)	0.1691(3)	0.3193(3)	0.4253(3)	3.11(9)
P(2)	0.0340(3)	0.4021(3)	0.2647(3)	2.95(8)
P(3)	−0.0425(3)	0.1646(3)	0.5433(3)	2.92(8)
P(4)	−0.2187(3)	0.2168(3)	0.4055(3)	2.96(7)
O(3)	−0.034(1)	−0.0199(8)	0.343(1)	5.7(3)
O(4)	0.234(1)	0.0662(9)	0.514(1)	6.2(3)
O(5)	0.197(1)	0.155(1)	0.215(1)	7.7(4)
O(6)	−0.072(1)	0.161(1)	0.168(1)	6.1(4)
C(1)	0.157(1)	0.399(2)	0.324(2)	9.0(5)
C(2)	−0.181(1)	0.184(1)	0.525(1)	3.6(3)
C(3)	0.001(2)	0.053(1)	0.364(1)	4.7(4)
C(4)	0.170(1)	0.106(1)	0.471(1)	3.7(3)
C(5)	0.144(2)	0.164(1)	0.284(1)	4.4(4)
C(6)	−0.075(1)	0.213(1)	0.231(1)	4.0(4)
C(11)	0.308(2)	0.297(2)	0.422(2)	6.6(6)
C(12)	0.163(2)	0.392(2)	0.528(2)	9.6(7)
C(21)	−0.005(2)	0.527(1)	0.261(2)	5.6(5)
C(22)	0.069(2)	0.384(2)	0.140(2)	7.0(6)
C(31)	−0.017(2)	0.236(1)	0.645(1)	5.4(5)
C(32)	−0.043(2)	0.043(1)	0.596(1)	5.6(5)
C(41)	−0.341(1)	0.282(1)	0.423(1)	5.3(5)
C(42)	−0.267(1)	0.106(1)	0.350(1)	4.6(4)

[a] *B* values for anisotropically refined atoms are given in the form of the isotropic equivalent displacement parameter defined as $B_{eq} = (8\pi^2/3)\sum_i\sum_j U_{ij}a^*_i a^*_j \mathbf{a}_i\cdot\mathbf{a}_j$.

the bands at 2035, 1954, and 1902 cm^{-1} are essentially the same as those in **3** while the remainder, especially that at 2010 cm^{-1},

Table 6. Positional and Thermal Parameters (Esd's in Parentheses) for $[Re(CO)_3(\mu\text{-}dmpm)_2Pt(PPh_3)]BrH_2O$ (**12**)

atom	*x*	*y*	*z*	B_{eq}[a] Å
Pt	0.22621(2)	0.05170(3)	−0.13695(1)	1.901(6)
Re	0.43340(3)	−0.04540(4)	−0.16560(1)	2.358(7)
Br	0.31311(9)	0.1603(2)	0.48406(4)	6.09(3)
P(1)	0.2489(2)	−0.0907(2)	−0.07997(7)	2.60(5)
P(2)	0.4903(2)	−0.1124(3)	−0.09498(8)	2.99(5)
P(3)	0.2496(2)	0.2402(2)	−0.17847(7)	2.42(4)
P(4)	0.4862(2)	0.1941(3)	−0.15843(7)	2.81(5)
P(5)	0.0350(2)	0.0763(2)	−0.12988(7)	2.07(4)
O(1)	0.6620(6)	−0.133(1)	−0.1926(3)	8.3(2)
O(2)	0.3695(8)	0.0122(9)	−0.2570(2)	6.2(2)
O(3)	0.3444(7)	−0.3364(8)	−0.1831(3)	6.2(2)
C(1)	0.5741(8)	−0.098(1)	−0.1822(3)	4.4(2)
C(2)	0.3900(8)	−0.004(1)	−0.2223(3)	3.6(2)
C(3)	0.3768(8)	−0.229(1)	−0.1752(3)	3.7(2)
C(4)	0.2220(8)	−0.272(1)	−0.0828(3)	4.0(2)
C(5)	0.1699(8)	−0.043(1)	−0.0344(3)	4.3(2)
C(6)	0.3861(8)	−0.078(1)	−0.0562(3)	3.2(2)
C(7)	0.5196(8)	−0.295(1)	−0.0905(3)	4.4(2)
C(8)	0.6140(8)	−0.038(1)	−0.0720(4)	5.3(3)
C(9)	0.1838(7)	0.258(1)	−0.2296(3)	3.8(2)
C(10)	0.2047(8)	0.389(1)	−0.1490(3)	3.6(2)
C(11)	0.3901(7)	0.2907(9)	−0.1910(3)	2.8(2)
C(12)	0.485(1)	0.285(1)	−0.1094(4)	5.1(3)
C(13)	0.6188(8)	0.241(1)	−0.1787(4)	5.5(3)
C(14)	−0.0402(6)	0.1472(9)	−0.1751(3)	2.4(2)
C(15)	−0.0714(7)	0.285(1)	−0.1761(3)	2.9(2)
C(16)	−0.1210(7)	0.343(1)	−0.2109(3)	3.5(2)
C(17)	−0.1434(8)	0.268(1)	−0.2460(3)	3.7(2)
C(18)	−0.1155(9)	0.132(1)	−0.2455(3)	4.8(3)
C(19)	−0.0635(9)	0.072(1)	−0.2118(3)	4.0(2)
C(20)	−0.0261(7)	−0.0954(9)	−0.1229(3)	2.6(2)
C(21)	−0.0904(7)	−0.132(1)	−0.0900(3)	3.2(2)
C(22)	−0.1290(8)	−0.263(1)	−0.0858(3)	4.4(2)
C(23)	−0.1054(9)	−0.362(1)	−0.1153(4)	5.1(3)
C(24)	−0.0378(9)	−0.330(1)	−0.1471(3)	4.5(2)
C(25)	0.0020(8)	−0.198(1)	−0.1513(3)	3.7(2)
C(26)	−0.0228(6)	0.1824(8)	−0.0893(2)	2.0(2)
C(27)	0.0441(6)	0.2560(9)	−0.0625(3)	2.6(2)
C(28)	−0.0013(8)	0.341(1)	−0.0325(3)	4.1(2)
C(29)	−0.1105(8)	0.355(1)	−0.0301(3)	4.1(2)
C(30)	−0.1795(7)	0.286(1)	−0.0572(3)	3.6(2)
C(31)	−0.1362(7)	0.1977(9)	−0.0856(3)	2.8(2)
O(4)	0.5865(5)	0.1521(9)	0.4880(2)	5.5(2)

[a] *B* values for anisotropically refined atoms are given in the form of the isotropic equivalent displacement parameter defined as $B_{eq} = (8\pi^2/3)\sum_i\sum_j U_{ij}a^*_i a^*_j \mathbf{a}_i\cdot\mathbf{a}_j$.

are comparable to those observed for *cis*-$Cr(CO)_4(dmpm)$.[23] By contrast neither **5** nor *fac*-$Cr_2(CO)_6(dmpm)_3$,[23] which contain the *fac*-$\{M(CO)_3\}$ (M = Mo, Cr) moiety, have bands due to this unit above 2000 cm^{-1}. The $^{31}P\{^1H\}$ NMR spectrum shows two resonances of equal intensity which can be analyzed as an AA′XX′ spin system with the higher field resonance appearing at a chemical shift comparable to that assigned to the coordinated phosphorus atoms in **3**. On this basis and its greater breadth, it is assigned to phosphorus bound to rhenium with the breadth due to the presence of the rhenium nuclear quadrupole.

With $Mo(CO)_3(CHT)$, **3** yields bright yellow, moderately soluble crystals analyzing as $ReMoBr(CO)_6(dmpm)_2$ (**5**). This composition and formulation of **5** as *fac*-$Re(CO)_3(\mu\text{-}Br)(\mu\text{-}dmpm)_2Mo(CO)_3$ has been confirmed by an X-ray crystal structure determination, and the spectroscopic data are in accordance with this.

Toluene solutions of **3** and $Co_2(CO)_8$ react with gas evolution to initially form an oily, dark brown solid. Recrystallization of the solid from acetone/diethyl ether and then acetonitrile/diethyl ether produced long orange needles analyzing as $ReCo_2$-

$Br(CO)_9(dmpm)_2$·MeCN (**6**). The $^{31}P\{^1H\}$ NMR spectrum

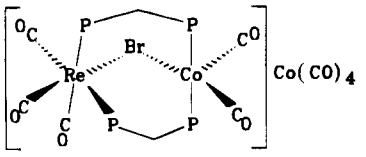

6

consists of two broad singlet resonances of equal intensity, the lower field of which is close to that found for $Co_2(CO)_4(dmpm)_2$ and is therefore assigned to dmpm coordinated to cobalt.[24] The upfield resonance, although at a lower chemical shift than most of the other complexes prepared here, is reasonably assigned to dmpm coordinated to rhenium. The infrared spectrum in the carbonyl region clearly shows two of three bands expected for the *fac*-{$Re(CO)_3$} moiety and an intense, broad band at 1892 cm^{-1} characteristic[25] of the $[Co(CO)_4]^-$ ion. On the basis of the behavior of **3** in this study, the observation of additional carbonyl absorptions, and the absence of $CoBr_2$ formation in the reaction, **6** is formulated as [*fac*-$Re(CO)_3(\mu\text{-}Br)(\mu\text{-}dmpm)_2Co(CO)_2$][$Co(CO)_4$], and this has been confirmed by an X-ray crystal structure study.

In an attempt to prepare a heterometallic complex containing a coordinated diolefin ligand, a solution of [Rh(COD)(acetone)$_x$]OTf, prepared in situ, was reacted with **3**. The $^{31}P\{^1H\}$ NMR spectrum of the resulting orange solution was exceedingly complex indicating the presence of several species. The distinct odor of free cyclooctadiene was also evident indicating at least some of these no longer contained the diolefin ligand. Following unsuccessful attempts to obtain characterizable products from this mixture, the initial reaction was repeated and the orange solution flushed with carbon monoxide from which a solid product consisting of a mixture of yellow and orange crystals was readily obtained. Recrystallization by vapor diffusion of diethyl ether into an acetone solution of the crude solid afforded a large quantity of bright yellow blocks (**7**) together with a small amount of dark orange rhombs (**8**), which were hand-separated under a microscope. Complex **7** analyzed

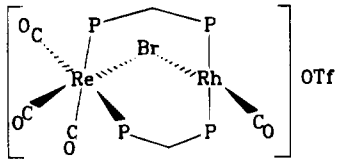

7

for [$ReRhBr(CO)_4(dmpm)_2$]OTf and exhibits an infrared spectrum in the carbonyl stretching region consisting of four bands, three of which compare well with those seen in **3** and indicate the presence of the *fac*-{$Re(CO)_3$} moiety. The fourth (1992 cm^{-1}) is consistent with a carbonyl ligand bound to a formally positively charged Rh(I) center. The $^{31}P\{^1H\}$ NMR spectrum of **7** consists of two resonances of equal intensity, the lower field of which is a doublet of triplets clearly indicating its assignment to phosphorus bound to rhodium. The upfield resonance appears as a triplet of doublets at a chemical shift characteristic of dmpm bound to rhenium. The small doublet splitting indicates a long range coupling of these phosphorus atoms to rhodium. On the basis of these data, **7** is formulated as [*fac*-$Re(CO)_3(\mu\text{-}Br)(\mu\text{-}dmpm)_2Rh(CO)$]OTf, and this has been confirmed by an X-ray crystal structure determination.

The dark orange crystals of **8**, obtained as the minor component from the above reaction, were not produced in

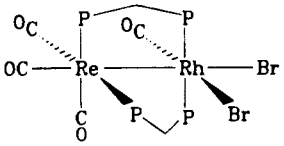

8

sufficient quantities to obtain analytical data. However, an X-ray crystal structure determination showed them to be *fac*-$Re(CO)_3(\mu\text{-}dmpm)_2Rh(CO)Br_2$ and the spectroscopic data are consistent with this. Thus the infrared spectrum (CH_2Cl_2 solution) shows bands at 2022 (vs), 1991 (m), 1921 (s), and 1904 (s) cm^{-1} which can be assigned to the {*fac*-$Re(CO)_3$} moiety and to a carbonyl ligand on a rhodium center with oxidation state above Rh(I). The $^{31}P\{^1H\}$ NMR spectrum (d_6-acetone) shows two signals of equal intensity, one at δ −3.2 (dt (^1J(Rh−P) = 93.5, ^2J(P−P′) = 41.9 Hz)) and the other at δ −35.3, which appears as an apparent quartet with splitting of *ca.* 42 Hz. The first can clearly be assigned to the phosphorus atoms bound to rhodium, and the lower value of ^1J(Rh−P) as compared with that seen for **7** is also consistent with the rhodium having a formal oxidation state higher than Rh(I). The second has a chemical shift comparable to the rhenium-bound phosphorus atoms in the other complexes reported here. The apparent quartet splitting is attributed to an additional coupling of these phosphorus atoms to rhodium with a coupling constant comparable in magnitude to that for ^2J(P−P′). This increased Rh−P′ coupling compared to that in **7** is consistent with the presence of the Rh−Re bond established by the structure determination.

The mechanism of formation of **8** has not been explored in detail, but we note that bromide loss from **3** occurs in the formation of **12** (vide infra) and complete transfer of bromide from rhenium to rhodium occurs when *fac*-$ReBr(CO)_3(\eta^1\text{-}MeN(PF_2)_2)_2$ reacts with Rh(I) complexes.[11] Thus Re−Br cleavage in **7** could occur to initially give a species with a terminal bromo ligand on rhodium followed by additional bromide abstraction from **3**, **7**, or a second molecule of the putative intermediate to give **8**.

An immediate precipitate forms on mixing toluene solutions of **3** and $PdCl_2(PhCN)_2$ which analyzes for $RePdBrCl_2(CO)_3(dmpm)_2$ (**9**). The insolubility of **9** in suitable solvents prevented

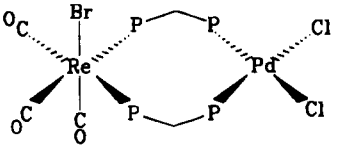

9

obtaining NMR spectra, but the infrared spectrum is clearly consistent with the retention of the *fac*-{$Re(CO)_3$} moiety. With the limited data available, a definitive determination of the structure is not possible, but that shown appears the most reasonable although a polymeric formulation, viz. [(dmpm)$ReBr(CO)_3$(dmpm)$PdCl_2]_n$ cannot be ruled out.

A facile reaction occurs between **3** and $Pt(C_2H_4)(PPh_3)_2$ from which a yellow-orange, microcrystalline solid could be obtained. The $^{31}P\{^1H\}$ NMR spectrum of this material ($CDCl_3$ solution) showed the presence of two dmpm-bridged Pt/Re complexes. One, **11**, is characterized by a pair of triplet resonances (^2J(P−

(24) Mirza, H. A.; Vitall, J. J.; Puddephatt, R. J.; Frampton, C. S.; Manojlovic-Muir, L.; Xia, W.; Hill, R. H. *Organometallics* **1993**, *12*, 2767.

(25) Edgell, W. F.; Lyford, J., IV. *J. Chem. Phys.* **1970**, *52*, 4329.

P) = 49.0 Hz) of equal intensity at δ −42.8 and −5.7, with the latter showing ^{195}Pt satellites (^1J(Pt−P) = 2882 Hz). The former resonance has a chemical shift comparable to those assigned to bridging dmpm bound to rhenium in the other complexes reported here, and its greater breadth confirms this assignment. The second species, **12**, is characterized by a set of multiplet resonances at δ −40.4, −15.1, and 18.5 in the intensity ratio 2:2:1 which can be analyzed as an AA′MM′X spin system. The chemical shift and breadth of the δ −40.4 resonance are consistent with its assignment to bridging dmpm bound to rhenium while the other two possess ^{195}Pt satellites. Also present in this spectrum is a sharp singlet at δ −4.7 which is assigned to free triphenylphosphine by comparison with an authentic sample under identical conditions. Recrystallization of the crude material results in a change in the proportions of **11** and **12** seen in the ^{31}P NMR spectrum, but a single species could not be obtained. Layering a nitromethane solution of the apparent mixture with diethyl ether results in the formation of dark orange rhombs and orange yellow plates. The former crystals become opaque and crumble on removal from the mother liquor, but the latter proved suitable for an X-ray structure determination which showed them to be [*fac*-Re(CO)$_3$(μ-dmpm)$_2$Pt(PPh$_3$)]Br·H$_2$O. This complex would be expected to exhibit three resonances in its ^{31}P NMR spectrum having a 2:2:1 intensity ratio and is thus identified as the species designated as **12** above with the resonances at δ −40.4 and δ

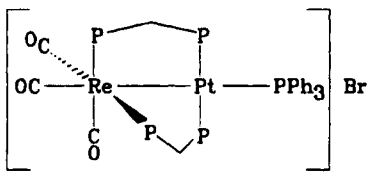

12

−15.1 assigned, respectively, to dmpm bound to rhenium and to platinum, while the δ 18.5 resonance is assigned to triphenylphosphine bound to platinum. The identity of **11** is less certain, but the intensity ratio and chemical shifts observed together with the absence of a resonance downfield of the phosphoric acid reference strongly indicate that **11** contains dmpm bridging platinum and rhenium but no triphenylphosphine. A reasonable formulation for **11** is therefore *fac*-Re-

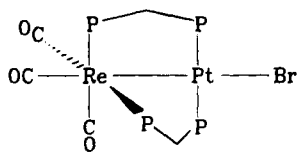

11

(CO)$_3$(μ-dmpm)$_2$PtBr. Interestingly the ^{31}P{^{1}H} NMR spectra ($CDCl_3$ solution) of hand-separated samples of the dark orange rhombs and the orange-yellow plates from which the crystal used for the structure determination of **12** was obtained are essentially identical and show **11** and **12** to be present in approximately equal amounts together with free triphenylphosphine. It thus appears that the bromide ion in **12** can partially replace triphenylphosphine to give an equilibrium mixture of **11** and **12**. What is not clear is the exact composition of the dark orange crystals since if they are pure **11** there would be no source of free triphenylphosphine to give the observed mixture of **11** and **12** in solution. We tentatively suggest that they may contain cocrystallized triphenylphosphine but have been unable to confirm this. The apparent lability of bromide and triphenylphosphine on platinum is confirmed by the addition

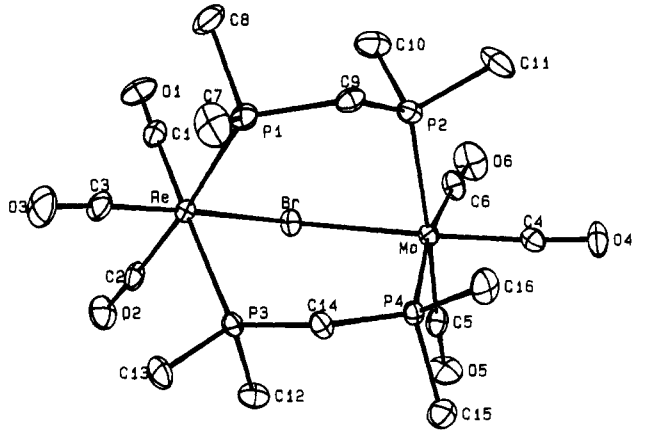

Figure 1. Perspective view of Re(CO)$_3$(μ-Br)(μ-dmpm)$_2$Mo(CO)$_3$ (**5**). Thermal ellipsoids are drawn at the 50% probability level, and hydrogen atoms are omitted for clarity.

of excess sodium tetraphenylborate to a methanol solution of the original solid obtained from **3** and Pt(C_2H_4)(PPh$_3$)$_2$ whose ^{31}P NMR spectrum showed the presence of **11**, **12**, and triphenylphosphine. Recrystallization of the orange precipitate obtained from dichloromethane/methanol provides orange crystals analyzing as [PtRe(CO)$_3$(dmpm)$_2$(PPh$_3$)]BPh$_4$·0.5CH_2Cl_2 (**10**) whose ^{31}P{^{1}H} NMR spectrum is identical to that initially assigned to **12** indicating the cation in **10** to have the same structure. No **11** or triphenylphosphine are evident.

The behavior of **3** in its reaction with low-valent transition metal complexes contrasts to some extent with that observed previously for the analogous *fac*-ReBr(CO)$_3$(η^1-MeN(PF$_2$)$_2$)$_2$.[11] With the latter, complete transfer of bromine from rhenium to the second metal has been found in all systems giving characterizable products, while **3** does so in only some cases. This is presumably due to the different electronic properties of the two diphosphine ligands.

Description of Structures. A common feature of the five structures is the {*fac*-Re(CO)$_3$P$_2$} moiety with the two phosphorus atoms of the bridging dmpm ligands *cis* to one another. The approximately octahedral coordination about rhenium is completed in **5**−**7** by a bridging bromine atom and in **8** and **12** by the second metal atom. The most significant departure from ideal octahedral geometry is seen in the P−Re−P angle (P(1)−Re−P(3) for **5**−**8** and P(2)−Re−P(4) for **12**), which is *ca.* 95° in **5** and **12** and *ca.* 102° in **6**−**8**. This is partly due to the greater bulk of dmpm as compared to that of the other ligands on rhenium but, particularly in **6**−**8**, also to the short backbone of dmpm coupled with the need of the other ends of these ligands to coordinate approximately *trans* to each other about the second metal. In **5**−**7**, the Re−C distances *trans* to phosphorus are significantly longer than that *trans* to bromine indicating a greater structural *trans* influence of the former ligand.

(a) *fac*-Re(CO)$_3$(μ-Br)(μ-dmpm)$_2$Mo(CO)$_3$ (5). A perspective view of **5** is shown in Figure 1, and pertinent distances and angles appear in Table 7. The crystal structure consists of the packing of the dinuclear molecules with no unusual intermolecular contacts. The coordination about molybdenum is also approximately octahedral with the Br−Re−P(1) and Br−Mo−P(4) angles significantly larger than Br−Re−P(3) and Br−Mo−P(2). The Re−Br distance compares favorably with the average of the Re−Br distances in Re$_2$(CO)$_6$(μ-Br)$_2$(μ-MeN(PF$_2$)$_2$) (2.640(1) Å),[11] while the Mo−Br distance lies at the

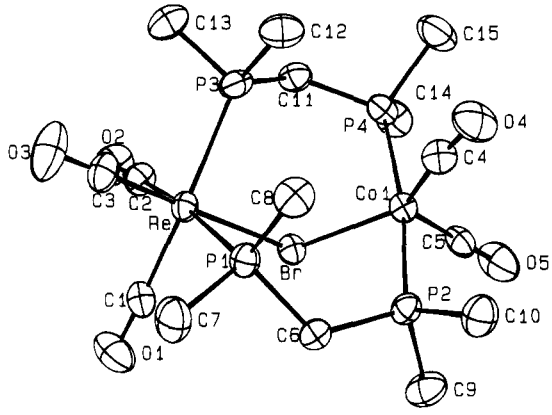

Figure 2. Perspective view of the $[Re(CO)_3(\mu\text{-}Br)(\mu\text{-}dmpm)_2Co(CO)_2]^+$ cation in **6**. Thermal ellipsoids are drawn at the 50% probability level, and hydrogen atoms are omitted for clarity.

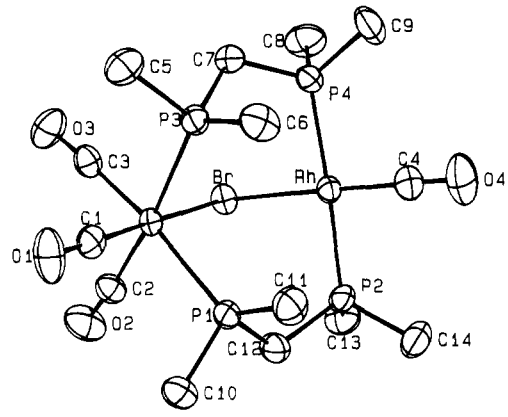

Figure 3. Perspective view of the $[Re(CO)_3(\mu\text{-}Br)(\mu\text{-}dmpm)_2Rh(CO)]^+$ cation in **7**. Thermal ellipsoids are drawn at the 50% probability level, and hydrogen atoms are omitted for clarity.

Table 7. Selected Bond Distances (Å) and Interbond Angles (deg) for $Re(CO)_3(\mu\text{-}Br)(\mu\text{-}dmpm)Mo(CO)_3$ (**5**)

	Distances		
Re–Br	2.650(1)	Mo–Br	2.744(1)
Re–P(1)	2.484(3)	Mo–P(2)	2.524(3)
Re–P(3)	2.456(3)	Mo–P(4)	2.518(3)
Re–C(1)	1.95(1)	Mo–C(4)	1.93(1)
Re–C(2)	1.95(1)	Mo–C(5)	1.96(1)
Re–C(3)	1.87(1)	Mo–C(6)	1.98(1)
	Angles		
Br–Re–P(1)	97.31(8)	Br–Mo–C(6)	89.4(3)
Br–Re–P(3)	88.05(7)	P(2)–Mo–P(4)	93.7(1)
Br–Re–C(1)	86.5(3)	P(2)–Mo–C(4)	93.7(3)
Br–Re–C(2)	88.5(4)	P(2)–Mo–C(5)	175.1(3)
Br–Re–C(3)	176.5(4)	P(2)–Mo–C(6)	89.0(4)
P(1)–Re–P(3)	95.0(1)	P(4)–Mo–C(4)	83.8(3)
P(1)–Re–C(1)	89.4(4)	P(4)–Mo–C(5)	89.8(4)
P(1)–Re–C(2)	174.0(3)	P(4)–Mo–C(6)	171.5(3)
P(1)–Re–C(2)	174.0(3)	P(4)–Mo–C(6)	171.5(3)
P(1)–Re–C(3)	86.2(4)	C(4)–Mo–C(5)	90.1(5)
P(3)–Re–C(1)	173.4(4)	C(4)–Mo–C(6)	88.0(5)
P(3)–Re–C(2)	86.6(3)	C(5)–Mo–C(6)	88.0(5)
P(3)–Re–C(3)	91.8(4)	Re–C(1)–O(1)	179(1)
C(1)–Re–C(2)	89.5(5)	Re–C(2)–O(2)	174(1)
C(1)–Re–C(3)	93.5(5)	Re–C(3)–O(3)	177(1)
C(2)–Re–C(3)	87.9(5)	Mo–C(4)–O(4)	176(1)
Br–Mo–P(2)	84.84(8)	Mo–C(5)–O(5)	177(1)
Br–Mo–P(4)	98.88(7)	Mo–C(6)–O(6)	176(1)
Br–Mo–C(4)	177.0(3)	Re–Br–Mo	117.89(4)
Br–Mo–C(5)	91.2(3)		

upper end of the range listed[26] for bromine bridging to molybdenum indicating the interaction with molybdenum to be weaker than with rhenium. The metal–metal separation of 4.622(1) Å is clearly too long for there to be any interaction between them.

(b) [*fac*-$Re(CO)_3(\mu\text{-}Br)(\mu\text{-}dmpm)_2Co(CO)_2$][$Co(CO)_4$]·MeCN (6). A perspective view of the dinuclear cation of **6** is shown in Figure 2, while relevant distances and angles are given in Table 8. The crystal structure consists of the packing of the dinuclear cations interspersed with $[Co(CO)_4]^-$ anions and solvent acetonitrile. There are no unusually short interionic contacts. The Re—Br distance is shorter than in **5** but still within the range of typical values.[26] The coordination about cobalt is best described as severely distorted trigonal bipyramidal. This is reflected particularly in the angles Br—Co(1)—C(4) (139.9(2)°) and P(2)—Co(1)—P(4) (169.06(7)°). The former is likely due to an attempt to avoid close contacts between the methyl groups built on C(8) and the carbonyl group {C(4)O(4)}. The

(26) Orpen, A. G.; Brammer, L.; Allen, F. H.; Kennard, O.; Watson, D. G.; Taylor, R. *J. Chem. Soc., Dalton Trans.* **1989**, S1.

Table 8. Selected Bond Distances (Å) and Interbond Angles (deg) for $[Re(CO)_3(\mu\text{-}Br)(\mu\text{-}dmpm)_2Co(CO)_2][Co(CO)_4]$·MeCN (**6**)

	Distances		
Re–Br	2.6283(6)	Co(1)–Br	2.4722(9)
Re–P(1)	2.461(1)	Co(1)–P(2)	2.214(2)
Re–P(3)	2.466(2)	Co(1)–P(4)	2.219(2)
Re–C(1)	1.941(7)	Co(1)–C(4)	1.721(7)
Re–C(2)	1.945(6)	Co(1)–C(5)	1.783(6)
Re–C(3)	1.881(6)		
	Angles		
Br–Re–P(1)	88.08(4)	Br–Co(1)–P(2)	87.35(5)
Br–Re–P(3)	88.75(4)	Br–Co(1)–P(4)	87.89(5)
Br–Re–C(1)	89.4(2)	Br–Co(1)–C(4)	139.9(2)
Br–Re–C(2)	91.3(2)	Br–Co(1)–C(5)	100.2(2)
Br–Re–C(3)	177.4(2)	P(2)–Co(1)–P(4)	169.06(7)
P(1)–Re–P(3)	101.09(5)	P(2)–Co(1)–C(4)	87.8(2)
P(1)–Re–C(1)	86.1(2)	P(2)–Co(1)–C(5)	94.7(2)
P(1)–Re–C(2)	173.8(2)	P(4)–Co(1)–C(4)	89.6(2)
P(1)–Re–C(3)	89.5(2)	P(4)–Co(1)–C(5)	95.8(2)
P(3)–Re–C(2)	85.0(2)	Re–C(1)–O(1)	176.8(6)
P(3)–Re–C(3)	90.8(2)	Re–C(2)–O(2)	176.5(6)
C(1)–Re–C(2)	87.8(3)	Re–C(3)–O(3)	179.0(7)
C(1)–Re–C(3)	91.3(3)	Co(1)–C(4)–O(4)	171.6(6)
C(2)–Re–C(3)	91.2(3)	Co(1)–C(5)–O(5)	174.0(6)
Re–Br–Co(1)	107.10(3)		

observed distances are as expected for normal van der Waals contacts and would therefore be considerably shorter were the Br—Co(1)—C(4) angle to adopt a more ideal value. The latter distortion is probably the result of the dmpm ligands having to coordinate *cis* on rhenium but *trans* on cobalt. The Co—Br distance is only slightly longer than those tabulated for terminal Co—Br bonds[26] indicating a relatively strong interaction with the formally positive cobalt center. Again, the metal—metal separation (4.104(1) Å) is too long for any direct interaction.

(c) [*fac*-$Re(CO)_3(\mu\text{-}Br)(\mu\text{-}dmpm)_2Rh(CO)$]OTf (7). A perspective view of the dinuclear cation of **7** is shown in Figure 3, and relevant distances and angles appear in Table 9. The crystal structure consists of the packing of the dinuclear cations and anions with no unusually short interionic contacts. The Re—Br distance is slightly longer than in the previous two structures but is still comparable to previously observed values.[26] The coordination about rhodium is very nearly square planar[27] with C(4) showing the greatest displacement (0.053(6) Å) from the mean coordination plane. The Rh—P distances compare favorably with those found in $[Rh_2(CO)_2(\mu\text{-}C_2R_2)(\mu\text{-}C_2R'_2)(\mu\text{-}$

(27) The weighted least squares plane containing Rh, Br, P(2), P(4), and C(4) has the crystallographic equation $7.0361x + 12.3558y - 5.2484z - 0.0329 = 0$. Distances of the constituent atoms from the plane (Å) are as follows: Rh, −0.0019(4); P(2), 0.010(1); P(4), 0.010(1); C(4), 0.053(6); Br, 0.0002(5).

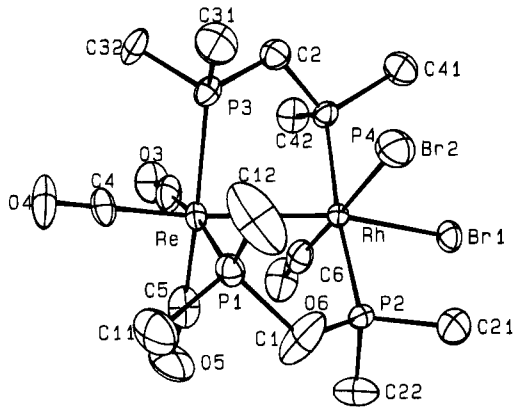

Figure 4. Perspective view of $Re(CO)_3(\mu\text{-dmpm})_2Rh(CO)Br_2$ (**8**). Thermal ellipsoids are drawn at the 50% probability level, and hydrogen atoms are omitted for clarity.

Table 9. Selected Bond Distances (Å) and Interbond Angles (deg) for $[Re(CO)_3(\mu\text{-Br})(\mu\text{-dmpm})_2Rh(CO)]OTf$ (**7**)

	Distances		
Re–Br	2.6674(5)	Re–C(3)	1.933(6)
Re–P(1)	2.480(1)	Rh–Br	2.5128(6)
Re–P(3)	2.473(1)	Rh–P(2)	2.312(1)
Re–C(1)	1.864(6)	Rh–P(4)	2.309(1)
Re–C(2)	1.952(6)	Rh–C(4)	1.803(6)
	Angles		
Br–Re–P(1)	91.41(3)	C(1)–Re–C(3)	89.6(2)
Br–Re–P(3)	91.58(3)	C(2)–Re–C(3)	88.5(2)
Br–Re–C(1)	178.8(2)	Br–Rh–P(2)	88.94(4)
Br–Re–C(2)	87.5(2)	Br–Rh–P(4)	88.36(4)
Br–Re–C(3)	90.3(2)	Br–Rh–C(4)	178.2(2)
P(1)–Re–P(3)	101.78(5)	P(2)–Rh–P(4)	177.24(5)
P(1)–Re–C(1)	88.5(2)	P(2)–Rh–C(4)	91.0(2)
P(1)–Re–C(2)	85.5(2)	P(4)–Rh–C(4)	91.6(2)
P(1)–Re–C(3)	173.8(2)	Re–Br–Rh	95.33(2)
P(3)–Re–C(1)	89.6(2)	Re–C(1)–O(1)	179.2(5)
P(3)–Re–C(2)	172.6(2)	Re–C(2)–O(2)	174.9(5)
P(3)–Re–C(3)	84.2(2)	Re–C(3)–O(3)	176.1(5)
C(1)–Re–C(2)	91.3(2)	Rh–C(4)–O(4)	178.0(6)

dmpm)$_2$] (R = CO_2Me, R′ = CF_3) (2.3080(8), 2.3132(8) Å),[28] while the Rh–Br distance is somewhat shorter than the mean (2.582(29) Å) of those previously observed[26] but only slightly longer than the shorter of the two terminal Rh–Br distances in **8** indicating a relatively strong interaction with the formally positive rhodium. The metal–metal separation of 3.8307(5) Å is shorter than those in **5** and **6**, presumably because of the smaller number of ligands on rhodium, but is still too long for any direct interaction.

(d) *fac*-$Re(CO)_3(\mu\text{-dmpm})_2Rh(CO)Br_2$ (8). A perspective view of **8** is shown in Figure 4, and pertinent distances and angles appear in Table 10. There are no unusually short intermolecular contacts in the solid. The Re–Rh distance of 2.893(1) Å is significantly longer than that found in $ReRh(CO)_4(\mu\text{-DPPM})_2$ (DPPM = bis(diphenylphosphino)methane) (2.7919(6) Å)[29] but is shorter than those found in $Re_2Rh(\mu\text{-H})(\mu_3\text{-}(Ph_2P)_2CH)(\mu\text{-}C_2Ph)(CO)_6(COD)$ (3.096(3), 3.163(3) Å)[30] as well as the intraligand P--P separations (P(1)--P(2) = 3.077(8), P(3)--P(4) = 3.070(8) Å). Thus an attractive metal–metal interaction is indicated. This could be described as either a normal covalent bond between 17-electron Re(I) and Rh(II) centers or as a donor bond from an 18-electron Re(0) to a 16-electron Rh(III) center. We are inclined to favor the former as

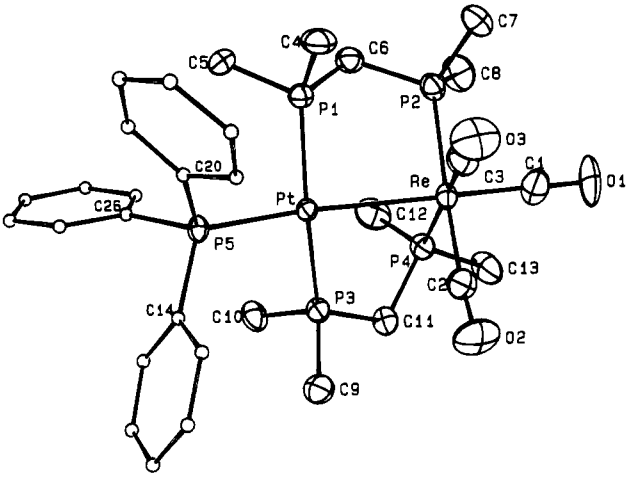

Figure 5. Perspective view of the $[Re(CO)_3(\mu\text{-dmpm})_2Pt(PPh_3)]^+$ cation in **12**. Thermal ellipsoids are drawn at the 50% probability level except for the phenyl carbon atoms, which are arbitrarily small for clarity. Hydrogen atoms are omitted.

Table 10. Selected Bond Distances (Å) and Interbond Angles (deg) for $Re(CO)_3(\mu\text{-dmpm})_2Rh(CO)Br_2$ (**8**)

	Distances		
Re–Ph	2.893(1)	Rh–Br(1)	2.723(2)
Re–P(1)	2.465(4)	Rh–Br(2)	2.508(3)
Re–P(3)	2.460(5)	Rh–P(2)	2.314(4)
Re–C(3)	1.94(2)	Rh–P(4)	2.304(4)
Re–C(4)	1.90(2)	Rh–C(6)	1.81(2)
Re–C(5)	1.91(2)		
	Angles		
Rh–Re–P(1)	85.1(1)	Re–Rh–P(2)	91.7(1)
Rh–Re–P(3)	85.8(1)	Re–Rh–P(4)	90.7(1)
Rh–Re–C(3)	97.6(6)	Re–Rh–C(6)	77.0(6)
Rh–Re–C(4)	168.0(5)	Br(1)–Rh–Br(2)	95.97(8)
Rh–Re–C(5)	95.2(6)	Br(1)–Rh–P(2)	87.8(1)
P(1)–Re–P(3)	102.9(1)	Br(1)–Rh–P(4)	92.6(1)
P(1)–Re–C(3)	170.9(7)	Br(1)–Rh–C(6)	85.9(6)
P(1)–Re–C(4)	87.4(5)	Br(2)–Rh–P(2)	86.7(1)
P(1)–Re–C(5)	83.9(6)	Br(2)–Rh–P(4)	83.7(1)
P(3)–Re–C(3)	86.1(7)	Br(2)–Rh–C(6)	178.1(6)
P(3)–Re–C(4)	86.9(6)	P(2)–Rh–P(4)	170.4(2)
P(3)–Re–C(5)	172.2(6)	P(2)–Rh–C(6)	93.7(6)
C(3)–Re–C(4)	91.3(8)	P(4)–Rh–C(6)	95.9(6)
C(3)–Re–C(5)	87.1(8)	Re–C(3)–O(3)	177(2)
C(4)–Re–C(5)	93.2(8)	Re–C(4)–O(4)	180(2)
Re–Rh–Br(1)	162.85(6)	Re–C(5)–O(5)	175(2)
Re–Rh–Br(2)	101.12(7)	Rh–C(6)–O(6)	175(2)

the CO stretching frequencies for the $\{Re(CO)_3\}$ unit are little different than those in **2**, while that for the carbonyl ligand bound to rhodium (1991 cm^{-1}) is intermediate between those typically found for neutral Rh(I) species, e.g. 1961 cm^{-1} in $RhBr(CO)(PMe_3)_2$,[31] and for neutral Rh(III) species, e.g. 2083 cm^{-1} in $RhBr_3(CO)(PEt_2Ph)_2$.[32] The Rh–Br(2) distance compares favorably with typical values[26] to a terminal bromine ligand, but that to Br(1) (2.723(2) Å) is considerably longer. This is considered to reflect a significant structural *trans* influence of the metal–metal bond which also is evident in the Re–C distances as the Re–C(4) distance is now comparable to that *trans* to phosphorus in contrast to what was seen in **5**–**7**. The coordination about both metals is approximately octahedral with that about rhodium showing both a twist about the P(2)--P(4) axis and a rotation about the metal–metal bond relative to the rhenium coordination sphere. The former twist is evident from

(28) Jenkins, J. A.; Cowie, M. *Organometallics* **1992**, *11*, 2774.
(29) Antonelli, D. M.; Cowie, M. *Organometallics* **1990**, *9*, 1818.
(30) Bruce, M. I.; Low, P. J.; Skelton, B. W.; White, A. H. *J. Chem. Soc., Dalton Trans.* **1993**, 3145.
(31) Browning, J.; Goggin, P. L.; Goodfellow, R. J.; Norton, M. G.; Rattray, A. J. M.; Taylor, B. F.; Mink, J. *J. Chem. Soc., Dalton Trans.* **1977**, 2061.
(32) Chatt, J.; Shaw, B. L. *J. Chem. Soc. A* **1966**, 1437.

Table 11. Selected Bond Distances (Å) and Interbond Angles (deg) for $[Re(CO)_3(\mu\text{-dmpm})_2Pt(PPh_3)]Br\cdot H_2O$ (**12**)

	Distances		
Pt−Re	2.8677(4)	Re−P(4)	2.429(3)
Pt−P(1)	2.303(2)	Re−C(1)	1.88(1)
Pt−P(3)	2.286(2)	Re−C(2)	1.92(1)
Pt−P(5)	2.364(2)	Re−C(3)	1.94(1)
Re−P(2)	2.441(3)		
	Angles		
Re−Pt−P(1)	87.64(6)	P(2)−Re−C(1)	86.6(3)
Re−Pt−P(3)	87.69(6)	P(2)−Re−C(2)	176.4(3)
Re−Pt−P(5)	160.67(6)	P(2)−Re−C(3)	89.8(3)
P(1)−Pt−P(3)	158.21(9)	P(4)−Re−C(1)	92.5(4)
P(1)−Pt−P(5)	95.27(8)	P(4)−Re−C(2)	87.6(3)
P(3)−Pt−P(5)	96.16(8)	P(4)−Re−C(3)	173.3(3)
Pt−Re−P(2)	91.83(6)	C(1)−Re−C(2)	91.7(4)
Pt−Re−P(4)	83.56(6)	C(1)−Re−C(3)	91.7(5)
Pt−Re−C(1)	175.7(4)	C(2)−Re−C(3)	87.1(4)
Pt−Re−C(2)	90.1(3)	Re−C(1)−O(1)	179(1)
Pt−Re−C(3)	92.3(3)	Re−C(2)−O(2)	174.7(9)
P(2)−Re−P(4)	95.62(9)	Re−C(3)−O(3)	176.4(9)

the Re—Rh—C(6) (77.0(6)°) and Re—Rh—Br(2) (101.12(7)°) angles, while the latter can be seen from the torsion angle P(3)—Re—Rh—P(4) of 33.8(2)°.

(e) [*fac*-$Re(CO)_3(\mu\text{-dmpm})_2Pt(PPh_3)]Br\cdot H_2O$ (12). A perspective view of the dinuclear cation in **12** is shown in Figure 5, and pertinent distances and angles appear in Table 11. There are no unusually short interionic contacts in the solid. The Pt—Re distance, 2.8677(4) Å, is shorter than that found in *fac*-$Re(CO)_3(\mu\text{-}MeN(PF_2)_2)_2Pt(Br)(PPh_3)$,[11] is somewhat longer than those for the unsupported Pt—Re bonds in $CpRe(H)(CO)_2Pt(H)(PPh_3)_2$ (2.838(1) Å)[33] and in *trans*-$Pt(CO)_2[Re(CO)_5]_2$ (2.8309(5) Å),[34] and is very close to that in $Re(N_2(p\text{-tol}))Cl(\mu\text{-}DPPM)_2PtCl$ (2.859(4) Å).[4] It is, however, significantly shorter than the intraligand P--P separations (P(1)--P(2) = 3.004(3), P(3)--P(4) = 2.986(3) Å) indicating the presence of an attractive metal—metal interaction. The lowering of the carbonyl stretching frequencies for the $\{Re(CO)_3\}$ moiety from those observed in the other complexes reported here suggests formulation of **12** as a Pt(I)/Re(0) species containing a formal single bond between the metals. Unlike *fac*-$Re(CO)_3(\mu\text{-}MeN(PF_2)_2)_2Pt(Br)(PPh_3)$,[11] the bromine is not coordinated to platinum but is present as Br^-, well-separated from the dinuclear cation. This is presumably the result of the more basic phosphine ligand present in **12**. The P(2)—Re—P(4) angle, 95.62(9)°, is considerably smaller than that found in **6**—**8** and is close to that seen in **5**. The closer approach to ideal octahedral geometry about rhenium is thus reflected in a greater distortion of the coordination about platinum from square planar, particularly in the P(1)—Pt—P(3) angle (158.21(9)°). Because of this, it is difficult to assess how much twist there is about the metal—metal bond but some indication is evident from the torsion angle (P(1)—Pt—Re—P(2) (22.82(8)°).

Acknowledgment. The support of the Tulane University Chemistry Department is gratefully acknowledged. We also thank Dr. Frank Fronczek for helpful discussions.

Supplementary Material Available: Full tables of data collection and refinement parameters, bond distances and interbond angles, calculated hydrogen atom positions and *B* values, anisotropic thermal displacement parameters, and rms amplitudes of anisotropic displacement (41 pages). Ordering information is given on any current masthead page.

(33) Casey, C. P.; Rutter, E. W., Jr.; Haller, K. J. *J. Am. Chem. Soc.* **1987**, *109*, 6886.
(34) Urbancic, M. A.; Wilson, S. R.; Shapley, J. R. *Inorg. Chem.* **1984**, *23*, 2954.